Egypt. J. Chem. **Vol. 63,** No. 12 pp. 5055 - 5070 (2020)

Egyptian Journal of Chemistry

http://ejchem.journals.ekb.eg/

Geochemical and Mineralogical Evaluation of Black Shale and its Hydrocarbon Potentiality, Southwest Sinai, Egypt

Esmat A. Abou El-Anwar,[a]*, Salman A. Salman,[a] Doaa Mousa,[b] Sami K. Aita[c]

[a] *Geological Sciences Dept., National Research Centre, PO Box 12622 Dokki, Giza, Egypt.*

[b] *Egyptian Petroleum Research Institute (EPRI), PO Box 11727, Nasr City, Cairo, Egypt*

[c] *Nuclear Materials Authority, P.O. Box: 530, Maadi, Cairo, Egypt*

Abstract

The investigation of new energy sources become one of the world tasks in the last decades. Oil shale is one of the promising energy sources and widespread in many parts of Egypt. So, this work was conducted to investigate hydrocarbon potentiality, geochemistry and environmental impact of Magharet El Maiah Formation black shale, Southwest Sinai. This shale is of Carboniferous age and composed mainly of kaolinite, montmorillonite and illite in a decreasing order with quartz and pyrite as non-clay minerals. They are deposited under oxic non-marine condition. Chemical analysis revealed that paleo-redox elements for the studied area were deposited under oxic environment and subjected to highly intensive chemical weathering. The calculated pollution indices indicated the mostly studied black shale isn't polluted. However, the studied black shale is enriched with some economic trace elements than the UCC and PAAS, especially Pb. All the studied samples are of indigenous origin. The organic richness of the studied samples ranges from fair to excellent total organic carbon content. The kerogen type is IV; the organic matter reaches the overmature stage and can be generate dry gas.

Keywords: Sinai; Black shale; Pollution; Kerogen; Palynofacies; Hydrocarbon Potentiality

1. Introduction

Exploration and development of unconventional energy resources is rapidly changing and constantly growing. Black shale has an international interest in exploiting hydrocarbons worldwide. Shale successful exploitation was mostly recorded in the USA, Canada and South America [1]. The retorting of oil shales to produce liquid hydrocarbons becomes an important alternative resource for energy [2]. The rapid advances in drilling technologies have led to the economic reevaluation of previously ignored organic rich shales for producing hydrocarbons. Successfully, hydrocarbon (especially gas) was achieved from organic shale in China and North America [3, 4].

Generally, organic matter of variable chemical composition and structure ranging from simple hydrocarbons to coal are widespread in rocks of sedimentary origin representing important reservoir of carbon between the exosphere and the deep Earth [5]. Quantitative assessment of source rocks and its hydrocarbons generation potentiality is an important issue, through determination of total organic carbon (TOC), Rock-Eval pyrolysis, vitrinite reflectance (R_0) and kerogen type determination. TOC is an important index and often used a proxy for organic matter abundance to evaluate the hydrocarbon quality of source rocks [6, 7]. The R_0 is used to predict thermal maturity of source rocks which represent an important parameter in the determination of hydrocarbon potentiality of source rock [8].

*Corresponding author e-mail: abouelanwar2004@yahoo.com
Receive Date: 01 October 2020, Revise Date: 20 November 2020, Accept Date: 29 November 2020
DOI: 10.21608/EJCHEM.2020.44732.2907

Sinai is the eastern gateway of Egypt, represents one sixth of Egypt area, and has strategic, historical and economic importance. Sinai contains many economic rocks and ores upon which many important industries are based. There are reliable trends for economic and social development of the Sinai Peninsula. The black shale deposits are one of those ores which occur within Carboniferous rocks (Paleozoic) in Southwest Sinai [9]. The carbonaceous shales in Sinai were studied by many authors; Temraz [9], Mostafa and Younes [10] and Ghandour et al.[11]. They are located at Ayun Mossa, Gebel Lefya, Gebel El-Maghara, as well as Abu-Zenima within West Central and North Sinai. This Carbonaceous shale is still needs more studies its qualifications and its suitability for hydrocarbon extraction or other applications.

In the present study nine (9) black shale samples were collected from Magharet El Maiah Formation at Wadi Budaa, Um Bogma, Sinai. This study focuses on the organic, inorganic and mineral composition of the collected samples to evaluate its hydrocarbon potentiality, their depositional environment and economic element enrichment.

2. Materials and Methods

2.1. Geologic Setting

The black shale in Sinai belongs to Paleozoic sediments. The Paleozoic sediments exposed above the basement rocks in most west central Sinai (Fig. 1a). These sediments divided into 6 rock units; Taba, Araba, Naqus, Um Bogma, Abu Thora and Abu Durba [12]. Abu Thora Formation is widely distributed in southwest Sinai especially in Um Bogma, Abu Durba area and Wadi Feiran, it is composed mainly of light colored sandstone with subordinate claystone, green to gray shale, thin coal seam, carbonaceous shale and siltstones beds. Abu Thora Group was subdivided into three formations by Soliman and El-Fetouh [13]; El-Hashash, Magharet El Maiah and Abu Zarab formations (Fig. 1b). Magharet El Maiah Formation thickness varies from 29 to 44.5 meter and composed of grey shale, carbonaceous shale, coal and sandstone. Carbonaceous shale and coal seam were considered as a source of REEs [14]. The carbonaceous shale is of fluvial origin [9].

Nine composite black shale samples were collect from the trenches dug by the Nuclear Materials Authority at Budaa area, Sinai (Fig. 1c). The thickness of shale layer in the excavated bit is about 2.5 meter (Fig. 1d).The radioactivity was measured on site with Geiger counter (RedEye B20-ER).

The mineral constituents of samples were investigated by the X-ray diffraction technique using a PANalytical X-ray Diffraction device (Model X'Pert PRO with Secondary Monochromator) at the Egyptian Mineral Resources Authority (Egypt). The SEM (Model Quanta FEG 250) was used to detect the morphology and the size of the sample constituents at the National Research Center laboratories. The chemical composition of nine samples was determined using XRF (Axios Sequential WD-XRF Spectrometer, Philips-PANalytical 2005) at the National Research Centre laboratories.

The samples were evaluated with organic geochemical analysis to determine their hydrocarbon potentiality. LECO SC632 was used for TOC and sulfur determination, Rock-Eval 6, HAWK and source rock analyzer for thermal pyrolysis at Stratochem service lab, Egypt. Five (5) selected samples of them were analyzed for palynofacies and Vitrinite Reflectance (R_0). Axio-Scope Transmitted light microscopy is used for kerogen typing and thermal alteration index (TAI) determination. According to organic geochemical evaluation, the samples were analyzed to determine: (1) Probable amount of produced hydrocarbons by determination of S1, S2 and TOC. (2) Kerogen Type by determination of the HI, OI ratios and palynomorph investigation. (3) Thermal maturity for the studied samples based on PI, T_{max}, and R_0.

To investigate the environmental impact of using this shale and its enrichment with trace elements; Index of Geoaccumulation (I_{geo}) [16], Enrichment Factor (EF) [17], Contamination Factor (CF), Degree of Contamination (DC) [18], and Pollution Load Index (PLI) [19] indices were calculated as following.

$$\mathbf{I_{geo} = Log_2 (C_m/1.5*B_m)}$$

$$\mathbf{EF = (C_m/B_m) / (R_s/R_c)}$$

$$\mathbf{CF = C_m/B_m}$$

$$\mathbf{DC} = \sum_n \boldsymbol{CF}$$

$$\mathbf{PLI} = \sqrt[n]{\boldsymbol{CF_1} * \boldsymbol{CF_2} * \dots\dots * \boldsymbol{CF_n}}$$

Where, C_m is measured concentration of target element, B_m is the concentration of the target element in the Upper Continental Crust [20]; As=4.8, Cr=92, Ni=47, Pb=17 and Zn=193 ppm. The 1.5 value is a constant used for discriminating the possible variations in the background data owing to the lithogenic impact. R_s is content of the reference element in the studied samples and R_c is content of the reference element in the Upper Continental Crust. In this study, zirconium was used as a conservative reference element to differentiate between natural and anthropogenic sources of elements owing to its natural lithogenic sources with no significant anthropogenic source [21]. Then is the number of the analyzed elements.

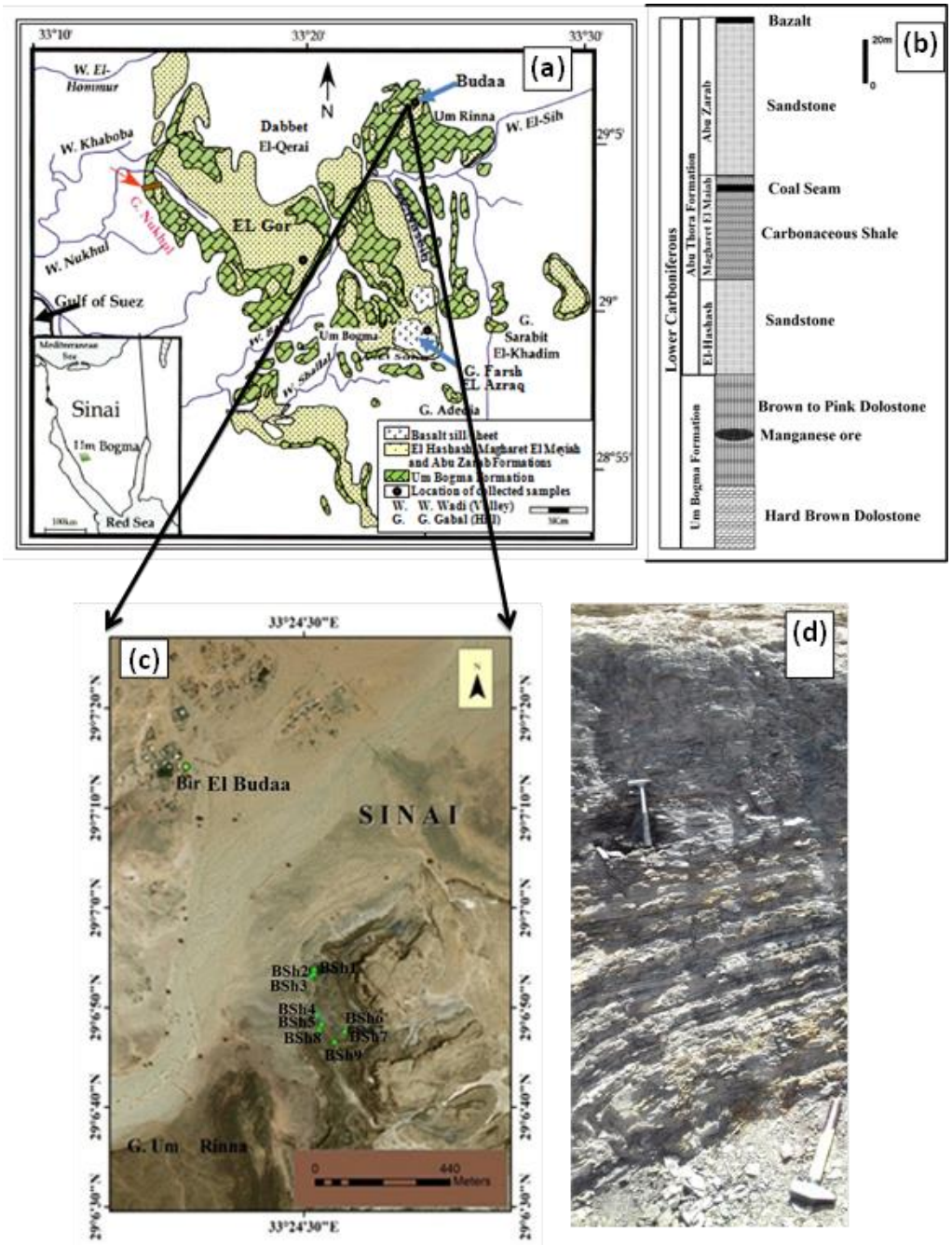

Fig. 1: (a) Geologic map [15], (b) Columnar section, (C) Satellite image showing the location of the study area and sampling sites (d) photo showing sampling black shale bed.

3. Result and discussion

3.1-Mineralogy

The X-ray diffraction analysis of four representative black shale samples (Fig. 2) collected from Budaa area, Sinai indicated the presence of clay minerals; kaolinite, montmorillonite and illite in decreasing order of abundance. The non-clay minerals are composed of quartz and pyrite. Kaolinite and quartz abundance in the studied samples can be referred to the deposition in non-marine (terrestrial) condition under warm/humid climate [22].

The montmorillonite was indicated by SEM examination (Fig. 3a). The dominance of kaolinite was also indicated by SEM examination. It deposited as detrital and authigenic origin (Fig. 3b). Figure (3b) shows kaolinite and framboidal pyrite. Framboidal pyrites are comprehensively pseudomorphosed and formed as authigenic, which conformed by X-ray diffractions. The framboids (4 μm) are pointed out the deposition of pyrite in reducing environments; which confirms with Abou El-Anwar and El-Sayed [23], Abou El-Anwar [24] and Abou El-Anwar et al. [25, 26]. Consequently, the vastly pyritic shale is deposited in euxinic environment. Pyrite as spheres is possibly representing shallow water.

3.2- Inorganic Geochemical investigation

3.2.1- Major and trace elements

The major and trace chemical compositions of the studied samples were illustrated in Table (1), whereas the major and trace interrelationship were given in Table (2). The measured radioactivity was 11 cps in all location indicating the low radiation hazard of these deposits.

The dominant major oxides SiO_2, Al_2O_3 and Fe_2O_3 (average 54.76, 18.36 and 4.65%; respectively), with SiO_2 lower than those in the Post Archaean Australian Shale (PAAS), while Al_2O_3% and Fe_2O_3% is enriched than the PAAS [20]. The prevailing of SiO_2 and Al_2O_3 oxides is argument on the presence of quartz and clay minerals as illustrated in Figure (2). The significant high concentration of SiO_2 may be attributed to detrital terrestrial coarser grained sediments in high energy environments [22, 27] However, the studied shale are relatively depleted in Ca and MgO%, and enrichment in, K_2O, TiO_2 and NaO_2% (Fig. 4a). The concentrations of Pb, Zn, Ni, As, Zr, and Cr in the studied samples were higher than the PAAS (Fig. 4b).

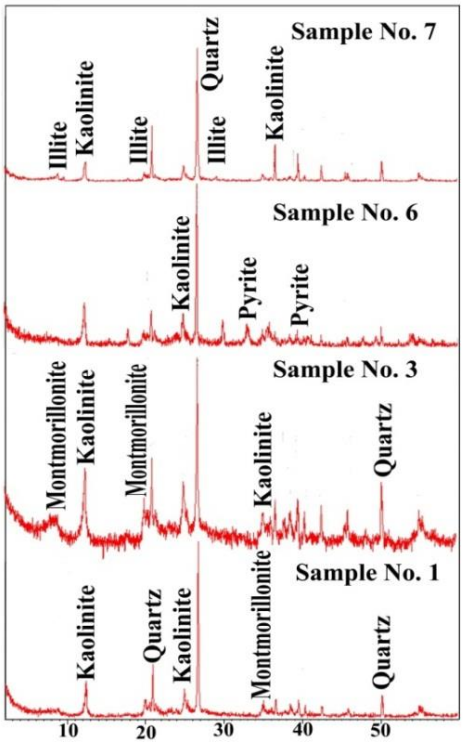

Fig. 2: X-ray diffractograms for the black shale of the studied area.

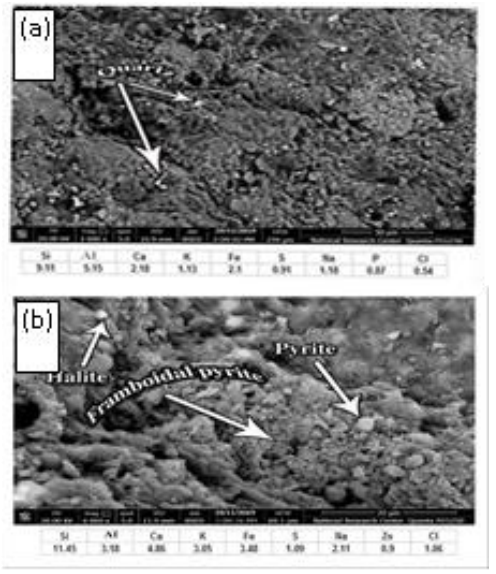

Fig. 3:BSE image and EDX analysis data showing (a) a well crystallized montmorillonite with well-developed morphology, and scattered quartz crystals in the matrix (b) a well crystallized kaolinite with well-developed morphology, spheres of framboidal pyrite (authigenic) and scattered halite crystals in the matrix.

Table 1:Major and trace elements content of the studied black shale.

S.N.	**SiO_2**	**TiO_2**	**Al_2O_3**	**Fe_2O_3**	**CaO**	**MgO**	**Na_2O**	**K_2O**	**P_2O_5**	**S**	**Cl**	**Sr**	**Ba**	**LOI**	**CIA**	**Mn**	Pb	Zn	Ni	Zr	As	Cr	Th
Unit	%															ppm							
1	64.82	4.77	10.71	2.64	0.3	0.23	0.05	0.74	0.4	0.02	0.03	0.08	0.01	15.23	90.8	85.3	371.3	24.1	62.9	1258.5	0.0	444.7	114.4
2	52.3	1.41	18.34	3.07	0.71	0.38	1.11	0.99	0.11	0.64	1.47	0.02	0.02	18.17	86.7	85.3	371.3	56.2	70.7	444.2	0.0	225.8	0
3	66.34	0.57	13.05	1.13	3.26	0.23	0.41	0.35	0.08	2.42	0.22	0.02	0.02	8.17	76.4	232.5	92.8	40.2	196.5	296.1	0.0	136.8	0
4	54.95	1.46	23.96	1.43	0.27	0.32	0.36	0.84	0.07	0.28	0.26	0.02	0.01	15.17	94.2	162.8	278.5	48.2	188.6	444.2	7.6	307.9	0
5	55.62	1.44	24.63	1.2	0.21	0.35	0.79	1.02	0.08	0.29	0.59	0.02	0.02	13.1	92.4	255.8	371.3	40.2	117.9	518.2	7.6	348.9	8.8
6	60.46	1.42	18.33	1.09	0.34	0.39	0.84	1.04	0.08	0.21	0.77	0.03	0.02	14.1	89.2	248.0	464.2	56.2	165.0	3183.3	159.1	390.0	79.2
7	56.13	1.53	19.56	1.09	0.57	0.29	1.12	1.01	0.08	0.5	0.96	0.02	0.02	16.58	87.9	240.3	278.5	48.2	196.5	592.2	189.4	164.2	44
8	28	0.8	16.56	26.23	2.37	0.24	0.27	0.83	0.05	1.59	0.1	0.02	0.02	20.22	82.7	170.5	1206.8	136.6	267.2	222.1	272.7	6.8	8.8
9	54.21	0.91	20.13	4.01	1.25	0.23	0.31	0.74	0.05	0.82	0.87	0.03	0.02	15.23	89.7	186.0	557.0	48.2	94.3	444.2	234.8	6.8	0
Min.	28	0.57	10.71	1.09	0.21	0.23	0.05	0.35	0.05	0.02	0.03	0.02	0.01	8.17	76.4	155.0	92.8	24.1	62.9	222.1	0.0	6.8	0
Max.	66.34	4.77	24.63	26.23	3.26	0.39	1.12	1.04	0.4	2.42	1.47	0.08	0.02	20.22	94.2	255.8	1206.8	136.6	267.2	3183.3	272.7	444.7	114.4
average	**54.76**	**1.59**	**18.36**	**4.65**	**1.03**	**0.30**	**0.58**	**0.84**	**0.11**	**0.75**	**0.59**	**0.03**	**0.02**	**15.11**	**87.8**	**155.0**	**443.5**	**55.3**	**151.1**	**822.6**	**96.8**	**225.8**	**0**

Table 2: Correlation matrix between the studied major and trace elements.

	SiO_2	TiO_2	Al_2O_3	Fe_2O_3	CaO	MgO	Na_2O	K_2O	P_2O_5	S	Cl	Sr	Ba	LOI	Pb	Zn	Ni	Zr	As	Cr	Th
SiO_2	1.00																				
TiO_2	0.37	1.00																			
$Al2O_3$	-0.21	-0.45	1.00																		
Fe_2O_3	-0.91	-0.21	-0.17	1.00																	
CaO	-0.23	-0.50	-0.46	0.46	1.00																
MgO	0.08	-0.14	0.54	-0.35	-0.59	1.00															
Na_2O	0.06	-0.33	0.41	-0.34	-0.32	0.74	1.00														
K_2O	-0.27	0.07	0.57	-0.03	-0.77	0.74	0.63	1.00													
P_2O_5	0.40	0.97	-0.63	-0.18	-0.30	-0.26	-0.40	-0.13	1.00												
S	-0.20	-0.58	-0.37	0.39	0.99	-0.50	-0.21	-0.74	-0.38	1.00											
Cl	0.06	-0.29	0.36	-0.34	-0.32	0.59	0.82	0.53	-0.34	-0.25	1.00										
Sr	0.37	0.93	-0.62	-0.13	-0.29	-0.35	-0.53	-0.15	0.95	-0.40	-0.38	1.00									
Ba	-0.26	-0.70	0.13	0.18	0.39	0.17	0.55	0.13	-0.64	0.44	0.52	-0.61	1.00								
LOI	-0.76	0.09	0.13	0.61	-0.28	0.11	0.12	0.59	-0.01	-0.32	0.24	0.00	-0.02	1.00							
Pb	-0.90	-0.16	-0.03	0.94	0.22	-0.20	-0.28	0.20	-0.18	0.14	-0.20	-0.06	0.21	0.71	1.00						
Zn	-0.94	-0.44	0.01	0.94	0.42	-0.11	-0.09	0.12	-0.43	0.39	-0.15	-0.39	0.34	0.62	0.90	1.00					
Ni	-0.51	-0.54	0.07	0.55	0.51	-0.18	-0.05	-0.14	-0.54	0.52	-0.40	-0.53	0.21	0.07	0.39	0.67	1.00				
Zr	0.34	0.26	-0.13	-0.27	-0.40	0.46	0.16	0.35	0.20	-0.44	0.08	0.31	-0.02	-0.11	-0.06	-0.17	-0.12	1.00			
As	-0.61	-0.36	0.06	0.59	0.21	-0.26	-0.02	0.19	-0.42	0.14	0.07	-0.21	0.46	0.49	0.71	0.65	0.46	0.09	1.00		
Cr	0.57	0.66	-0.01	-0.55	-0.68	0.50	0.09	0.32	0.59	-0.68	-0.10	0.50	-0.53	-0.23	-0.46	-0.58	-0.43	0.58	-0.64	1.00	
Th	0.38	0.81	-0.51	-0.19	-0.42	-0.01	-0.14	0.18	0.77	-0.51	-0.23	0.81	-0.39	0.02	-0.07	-0.30	-0.27	0.69	-0.03	0.64	1.00

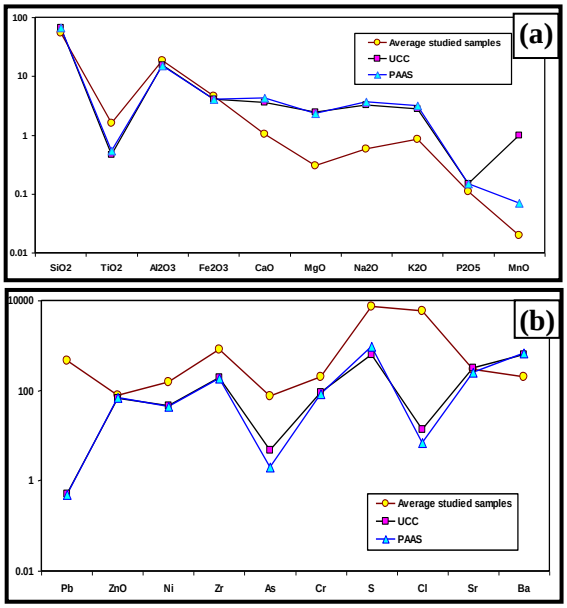

Fig.4: Comparison of resulted (a) major oxides (b) trace elements with the PAAS [20] and UCC [28].

The high loss on ignition, varies from 8.17 to 20.22% (average 15.11%), indicate the great quantities of organic matter. The loss on ignition strong positive correlation with K_2O (r= 0.60) indicated the dominated of clay minerals as confirmed SEM and XRD results. The negative relation between SiO_2 and Al_2O_3 (r = -21) indicated that the majority alumina is nearby as clay minerals, which confirmed with SEM examination (Table 1) and silica appears as quartz. Fe_2O_3 is averaged (4.65%) this percentage could be related the effect of the hydrothermal escape or additions of Fe, reliable with reduced fluids. Iron relatively high concentrations may be attributed to the presence of pyrite (Figs. 2 and 3). Anomalous values may be resulted from the presence of iron oxides as cement materials in these deposits [12]. The positive relation between Fe_2O_3 and total sulfur (r = 0.39) revealed that the organic sulfur prevails beside with pyrite, which confirmed by XRD and SEM examinations [24, 26].The measured sulfur (S wt%) of the studied samples is low with an average value 0.75% (Table 1), that is argument for a terrestrial sedimentation [29] with organic and inorganic (pyrite, Figs. 2 and 3) sources of S.

Zr, Cr and Th are positive correlated with SiO_2 (r= 0.34, 0.57 and 0.38; respectively), Table (2). This indicates that these trace elements associated with detrital quartz. Th is also, positive correlated with Zr and Cr (r= 0.69 and 0.64; respectively) which revealed that Th can also associated with heavy metals. Pb, Zn, Ni and As are positive correlated with Fe_2O_3(r=0.94, 0.94, 0.55 and 0.59; respectively), this indicated that these elements associated with iron oxides (Table 2).

The concentration of Sr and Ba is relatively low in the studied samples (Table 1) indicating non-marine; freshwater environment [22]. This is supported by the absence of Co and relatively low concentration of Ni [29] which is strongly indicative of terrestrial deposition under oxic conditions. This result is online with Temraz [9] who point to the fluvial depositional condition of this shale.

Generally the chemical data are compatible with the XRD results and the major element comparable with the mineralogical variations compositions (see Section 4.3). The higher amounts of Si and Al in the studied samples with the mineralogical assemblage indicate the prevalence of a humid-warm climate [30].

3.2.2- Redox-sensitive elements

Percentage of redox-sensitive elements (Cd, Cr, Cu, Ni, Mo, Re, Sb, U and V) can give good indication about paleo-environments [26, 31, 32]. These elements are generally enriched in anoxic environment as a result of oxygen depletion and vice versa for oxic environment [31]. The relative low concentration of the recorded redox-sensitive elements (Cr, Ni, Th) and the absence of U, Co, V in the studied sample indicated the oxic depositional condition. Pattan and Pearce [33] mentioned that sediment with less than 4 ppm U is deposited in oxic conditions. According to Lewan [34] the dominance of Ni over V (not detect) in the studied samples indicated the oxic environment of deposition.

3.2.3-Chemical mobility and weathering trends

In a sedimentary basin, the chemical composition of the weathering products is related to the mobility of different elements through weathering [35]. Sediments chemical weathering strength can be

estimated by appling the chemical index of alteration (CIA) equation[36].

$$\mathbf{CIA=[Al_2O_3/ (Al_2O_3+CaO^*+Na_2O +K_2O)X100]}$$

where CaO* represents CaO associated with the silicate minerals of the sample. The CIA values in the investegated shalevary from 76.4 to 94.2% and averaging 87.8% (Table 1). This value indicate that the source of the principal minerals was feldspars and/or mafic rocks and, commonly, represents highly intensive chemical weathering [26, 36].

3.2.4- Pollution

The economic value of black shales, not only attributed to its potentiality as oil-producing rocks but also as a source of some trace elements [37, 38]. Black shales are important as syngenetic hosts for metal deposits; as Kupferschiefer black shale in Central Europe that enriched with Cu and Pb, Oklo black shale in Africa contain concentration of U. In Sweden, Alum shales have been used as a source of pyrolysis oil and uranium [39, 40]. Also, it is contains considerable concentrations of redox sensitive metals (e.g. V, U, Mo, Ni, Re) and other economic elements; Cu, Pb, Zn, Au, Hg, Sb etc… [41, 42, 43]. So, contamination indices are used to assess the heavy metals enrichment [44, 45, 46, 47].

The calculated EF values indicated that shales of the studied area are nearly free from As, only one sample was extremely enriched with it (Table 3). This sample was exposed and subjected to the impact of the surrounding igneous rocks which may be the reason for As enrichment. Chromium is almost minimum to moderate enriched in the studied samples. Nickel is also low to moderate enriched in the studied black shale. The studied samples are generally enriched with Pb from moderate to extreme enrichment degree. The EF values indicated the depeltion of Zn in the studied samples.

The calculated geoaccumulation index with respect to As; 3 samples were uncontaminated, 2 samples were uncontaminated to moderately contaminated, 2 samples were strongly to extremely contaminated and 2 samples were extremely enriched (Table 3). Three samples were uncontaminated with Cr, two samples are uncontaminated to moderately contaminated and the other samples are moderately with Cr. With respect to Ni, one sample was uncontaminated to moderately contaminated, one sample was extremely contaminated, 4 samples were moderately to strongly contaminated, 3 samples were moderately contaminated. The I_{geo} of Pb ranged from 1.9 (Moderately contaminated) to 5.6 (Extremely contaminated). The I_{geo} of Zn indicted that was uncontamination with respect to Zn.

The calculated contamination factor (Table 3) indicates that all the black shale samples were very high contaminated with Pb (CF > 6) and only 4 samples with As. With respect to Cr, one sample had low CF three samples had moderate CF and 3 samples had considerable CF. Ni was of moderate CF in 4 samples and 5 samples had considerable CF. Zn shows low CF in the studied samples (CF<1).

According to the DC values (Table 3) one sample was of moderate DC, 4 samples were of considerable DC and 4 samples were of very high DC. CF high values for As and Pb reported in the studied black shale samples led to the wide band of high contamination category in the samples. PLI is presented in Table (3) indicated that the studied black shale samples were not polluted (PLI < 1) in three samples and polluted in the other samples (PLI > 1). In addition to the calculated indices, the comparison with the world black shale (Table 4) indicted that the studied shale contain elevated trace elements in some samples than the world shale especially Pb.

3.3- Organic geochemistrey

The evaluation of hydrocarbon potentiality for the studied black shale samples using Total Organic Carbon (TOC), Sulfur (S)%, Rock-Eval pyrolysis and microscopic studies (palynofacies and Vitrinite Reflectance (R_0)) will be discussed in this section.

3.3.1- The organic matter quantity (organic richness)

Organic richness of rock samples can be determined using the weight percent of total organic carbon "TOC". Organic richness determined the organic carbon content in both kerogen and bitumen fractions. In the investigated shale, the TOC is high and varied from 0.7 to 7.51% (Table 5). In petroleum industry source rocks with more than 2% TOC is considered of very good hydrocarbon potential source rock while those over 4% TOC is considered as excellent potential source rock (Table 6). On the

Table 3: Pollution indices values of the studied black shales

	Enrichment factor (EF)					Geoaccumulation index (I_{geo})					Contamination Factor (CF)					Degree of Contamination (DC)	Pollution load index (PLI)
	As	Cr	Ni	Pb	Zn	As	Cr	Ni	Pb	Zn	As	Cr	Ni	Pb	Zn		
1	0.0	0.7	0.2	3.3	0.1	0.0	1.7	0.9	3.9	-2.1	0.0	4.8	1.3	21.8	0.4	28.4	0.0
2	0.0	1.1	0.7	9.5	0.4	0.0	0.7	1.1	3.9	-0.8	0.0	2.5	1.5	21.8	0.8	26.6	0.0
3	0.0	1.0	2.7	3.6	0.4	0.0	0.0	2.6	1.9	-1.3	0.0	1.5	4.2	5.5	0.6	11.7	0.0
4	0.7	1.5	1.7	7.1	0.3	0.1	1.2	2.5	3.4	-1.1	1.6	3.3	4.0	16.4	0.7	26.0	3.0
5	0.6	1.4	0.9	8.1	0.2	0.1	1.3	1.8	3.9	-1.3	1.6	3.8	2.5	21.8	0.6	30.3	2.9
6	2.0	0.3	0.2	1.7	0.1	4.5	1.5	2.3	4.2	-0.8	33.1	4.2	3.5	27.3	0.8	69.0	6.5
7	12.9	0.6	1.4	5.3	0.2	4.7	0.3	2.6	3.4	-1.1	39.4	1.8	4.2	16.4	0.7	62.5	5.1
8	49.4	0.1	4.9	61.7	1.8	5.2	-4.3	3.0	5.6	0.4	56.8	0.1	5.7	71.0	2.0	135.6	5.1
9	21.3	0.0	0.9	14.2	0.3	5.0	-4.3	1.5	4.4	-1.1	48.9	0.1	2.0	32.8	0.7	84.5	2.8

Table 4: Comparison between the current study and the world shale (ppm).

element	Current study	UCC [28]	North American Shale Composite (NASC)[49]	Average shale[50]	Black shales US and Canada[51]	Black shales worldwide (median)[52]	background worldwide [52]
As	Bdl - 272.7	4.8	28.4	13	-	30	10-80
Cr	6.8 – 444.7	92	124.5	90	100	96	50-160
Pb	92.8- 1206.8	17	-	20	20	21	10 - 40
Ni	62.9- 267.2	47	58	68	50	70	40-140
Zn	24.1 - 136.6	193	-	95	<300	130	60–300

UCC: Upper Continental Crust

Table 5: Rock-Eval pyrolysis data of the studied samples from Magharet El MaiahFm., Budaa area, Sinai.

sample no.	TOC	S1	S2	S3	T_{max}	HI	OI	GP	PI	$S_{organic}$	R_0%
	Wt. %	mg/g	mg/g	mg/g						Wt.%	
1	5.09	0.03	0.26	4.95	490	5	97	0.29	0.10	0.79	1.03
2	4.48	0.03	0.12	3.96	515	3	88	0.15	0.20	0.43	1.08
3	3.34	0.02	0.12	4.30	488	4	129	0.14	0.14	0.55	-
4	2.70	0.02	0.16	2.38	484	6	88	0.18	0.11	0.29	1.11
5	2.03	0.02	0.17	2.56	496	8	126	0.19	0.11	0.25	1.11
6	7.51	0.02	0.08	6.87	508	1	91	0.1	0.20	4.14	-
7	4.65	0.02	0.13	3.95	602	3	85	0.15	0.13	0.40	1.33
8	0.70	0.02	0.06	2.38	515	9	339	0.08	0.25	1.22	-
9	1.87	0.02	0.07	2.16	606	4	116	0.09	0.22	0.23	-

TOC = Total organic carbon, wt %; S1: Free hydrocarbons content, mg HC/g rock; S2: Remaining hydrocarbons generative potential, mg HC/g rock; S3: Carbon dioxide yield, mg CO_2/g rock; HI: Hydrogen index = 100×S2/ TOC (mg HC/TOC); OI: Oxygen index =S3×100/ TOC, mg CO_2/g TOC; T_{max} = Temperature at maximum of S2 peak; GP: Generative potential = S1+S2; PI: Production index = S1 / (S1+S2), S: $S_{organic}$: organic sulfur wt%.

Table 6: Geochemical Parameters Describing the Petroleum Potential (Quantity) [53].

Petroleum Potential	TOC (wt %)	Rock-Eval pyrolysis	
		S1	S2
Excellent	> 4	> 4	> 20
Very good	2 - 4	2 - 4	10 – 20
Good	1 – 2	1 – 2	5 – 10
Fair	0.5 – 1	0.5 – 1	2.5 – 5
Poor	0 – 0.5	0 -5	0 – 2.5

other hand rocks with more than 10% TOC are of little value and often considered too immature for development [48]. The studied samples data are represented in (Table 6) and according to the above discussion the organic richness of the studied samples ranges from fair to excellent total organic carbon content (Fig. 5a).

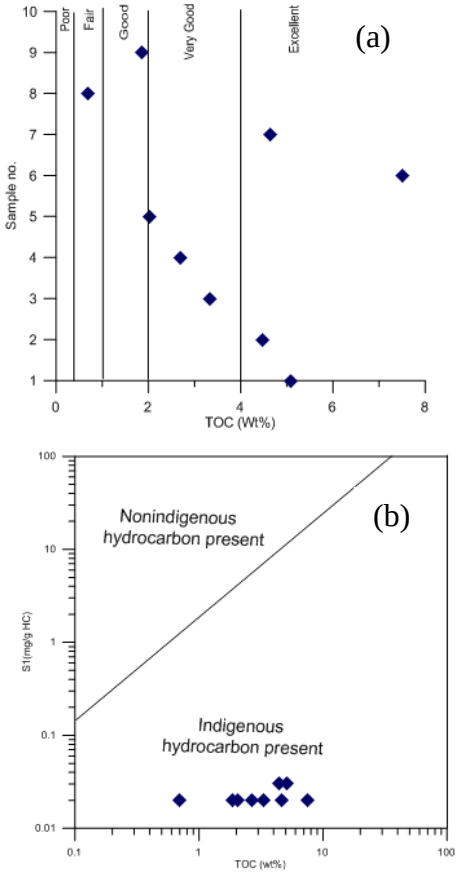

Fig. 5: (a) TOC content classes of the studied samples (b) TOC vs. S1 for the studied samples [57].

As shown in Figure (5b), the cross plot of S1 versus TOC (wt%) is commonly used to discriminate migrated hydrocarbons and contaminated from indigenous hydrocarbons [54]. All the studied samples show indigenous origin. Even though the importance of TOC, the source rock generative potential is mainly determined by S2 value (the produced hydrocarbon amount during sample pyrolysis). The studied samples have S2 values less than 1 mg/g indicating the poor possibility of hydrocarbon generative according to Peters and Cassa [53]. The poor generative potentiality is also indicated from the low GP and PI values (less than 1) in all samples. The S2 value can be used with TOC to predict the type of kerogen as shown in (Fig. 6), the kerogen type is III.

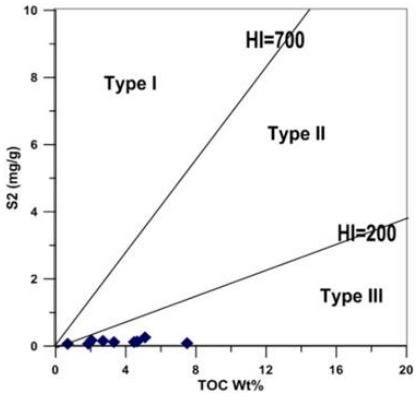

Fig.6: TOC vs. S2 for the studied samples [58]..

TOC also used vs total sulfur content to illustrate the environment of deposition (Fig. 7), which revealed that the OM deposited mostly in non-marine environment [55] under oxic to suboxic conditions [56].

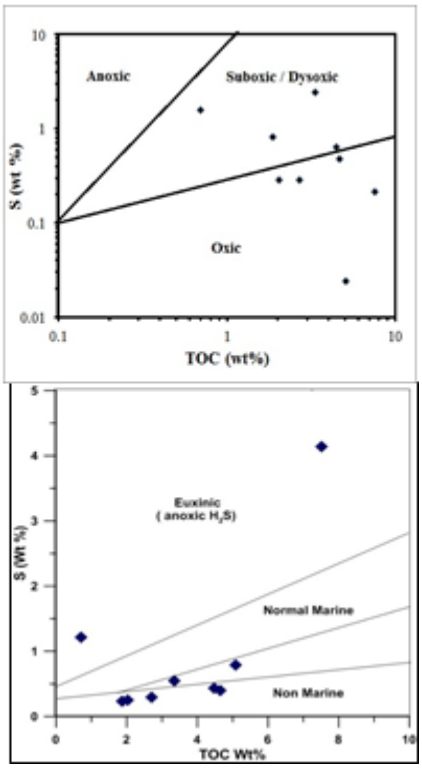

Fig.7: TOC vs. S content to determine depositional environment [55].

It is appears that organic sulfur (Table 5) is generally less than the total sulfur (Table 1) content of the studied samples. this indicate the presence of another source of sulfur in samples; iron sulfides (pyrite) as shown in figures (2 and 3) and supported by the negative correlation between total sulfur and TOC content.

3.3.2- Organic matter (kerogen) types

The type of kerogen found in the organic matter plays an important role in hydrocarbon generation. Kerogen (insoluble organic matter) represents the organic matter found in the sedimentary rocks which is not soluble in organic solvents. Kerogen has many types due to the variation of chemical composition of organic matter [7].

Organic matter can be classified into three major kerogen types:

1- Kerogen type (I and II) which have sapropelic type forming (oil prone) from marine and terrestrial origin.

2- Kerogen type (III) which is humic type derived from land plant with its parts lignine and cellulose and forming (gas-prone).

3- kerogen type(II/III or III/II) which is a mixed type from the previous one [59].

Many parameters from the Rock-Eval 6 analyzer are used to determine the kerogen type, the level of thermal maturation and oxygen richness. From these parameters the hydrogen index (HI) and oxygen index (OI). HI vs. OI is used to determine the kerogen type and level of thermal maturation [60].

Peters and Cassa [53] arrange the HI value as <150 represent gas-prone organic matter, HI value from 150-300 represent gas-oil-prone organic matter and HI >300 represent oil-prone organic matter (Table 5).

According to Tissot and Welte [61] and Pitman, et al. [62] elucidated the relation between HI and thermal maturity, as in low level of thermal maturation (R_0 less than 0.5%) HI is low, in case of kerogen type I and II (oil-prone) Hydrogen Index is more than 400 mg HC/g TOC and OI<50 mg CO_2 /g TOC. Kerogen type III (gas-prone) have low hydrogen index <200 mgHC/g TOC and a range of OI from 5-100 mg CO_2 /g TOC.

Kerogen Type IV is thermally mature with vitrinite reflectance more than 0.75% and HI less than 300 mg HC/g TOC.

In the studied samples the HI values for the analysed samples is low ranges from 1 to 9 with high OI ranges from 85-339 (Table 5), this results indicating kerogen type III or IV,(Table 7and Fig. 8). This result is confirmed with the plot of T_{max} vs HI in (Fig. 9).

Table 7: Geochemical parameters describing kerogen type (quality) and the character of expelled products [53].

Kerogen Type	S2/S3	Main expelled at peak maturity
I	> 15	Oil
II	10-15	Oil
II/III	5-10	Mixed oil+gas
III	1-5	Gas
IV	< 1	None

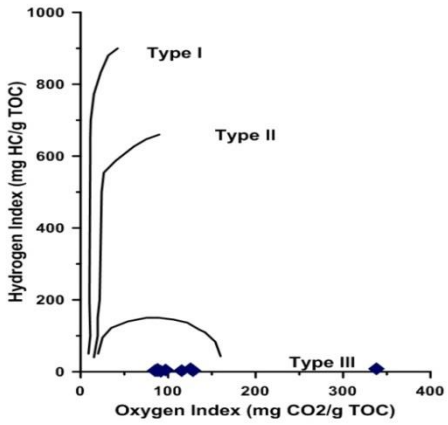

Fig. 8: HI versus OI of the studied samples [63].

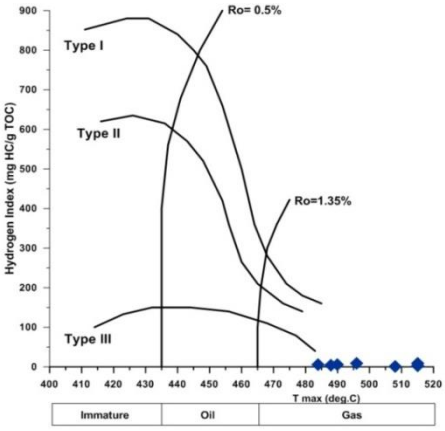

Fig. 9: T_{max}vs. HI showing the kerogen type [64].

3.3.3- Thermal maturation

Rock-Eval pyrolysis parameters, T_{max} and production index (PI), are used to represent the thermal maturation of organic matter (Table 8). Immature organic matter has PI value less than 0.1 , at the bottom of the oil window this ratio reaches about 0.4 and when the hydrocarbons generative

potential capacity of the kerogen has been exhausted, this ratio increases to 1 [65]. It has also been indicated that T_{max} values can be correlated with the vitrinite reflectance for Type-III kerogen and humic coal [66, 67].

Vitrinite reflectance (R_0), thermal alteration index (TAI) are another important maturity indicator as shown in (Table 8). R_0 is one of the most reliable maturation indicators and has been applied frequently [68, 8]. The R_0 is directly proportional with thermal maturity owing to increasing the aromatic units stacking resulted from aromatization and condensation elevation of the molecular structure [69]. It is generally known that the commercial oil generation begins at R_0 value between 0.6 and 0.65[70] as shown in (Table 8).

The T_{max} value for the studied samples ranges from 484-606^{o}C (Table 6) which indicates mature to post mature stage as shown in (Fig. 10a), and the relation between the PI and T_{max} (Fig. 10b) shows that the organic matter reaches the overmature stage and may produce dry gas.

Table 8: Geochemical parameters describing the level of thermal maturation [53].

Stage of thermal maturation		Maturation			Generation
		R_0 (%)	T_{max} (^{o}C)	TAI	PI[S1/ (S1 +S2)]
Immature		0.2-0.6	<435	1.5-2.6	<0.05
Mature	**Early**	0.60-0.65	435-445	2.6-2.7	0.10-0.15
	Peak	0.65-0.90	445-450	2.7-2.9	0.25-0.40
	Late	0.90-1.35	450-470	2.9-3.3	—
	Post-mature	>1.35	>470	>3.3	—

3.3.4- Palynofacies analysis

According to Tyson [72], the main objectives of microscopic investigation of palynofacies are to detect the origin of the organic matter, different components relative percent and preservation state, the hydrocarbons generating potential of the OM, the degree of its thermal alteration, the nature of the depositional paleo-environment and the oxidation-reduction conditions.

Regarding the kerogen microscopy analysis the most interest thing is the shape and color of the sporomorphs (spores and pollen grains), as the color reflect the Thermal Alteration Index (TAI). Regarding the TAI maturity scale, there are at least 5 different scales for the TAI. The most common/famous scales for petroleum exploration are the Chevron, Staplin, Roberson and geochemical labs scale (Table 9).

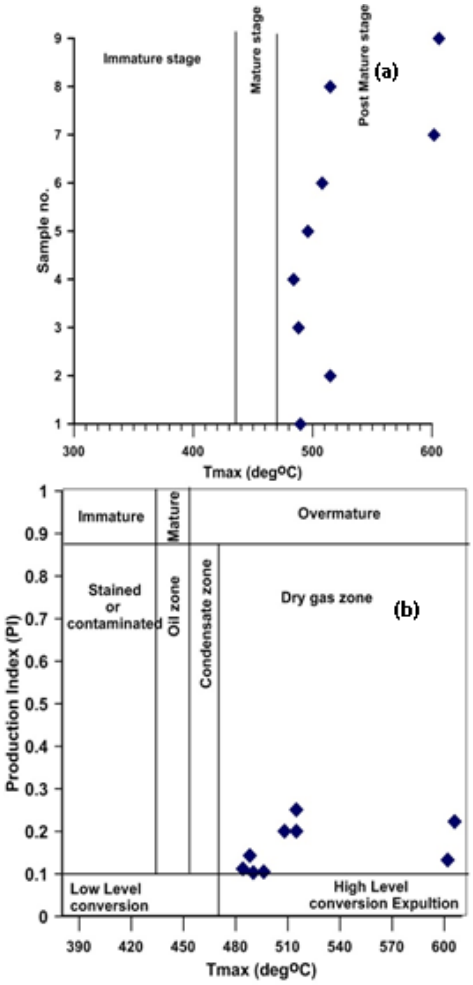

Fig. 10: (a) Plot of T_{max} in the studied samples, (b) Cross plot of T_{max} vs PI modified from [71].

It is can be also used to recognized the kerogen type as mentioned by Tyson [72, 73].

1. Type-I kerogen (highly oil-prone material) consists of algal material originated from closed basins, lagoons and lakes. It has the ability to generate oil.
2. Type-II kerogen (oil-prone material) consists of sapropelic OM deposited in anoxic marine environments. This kind of kerogen has the ability to produce both oil and gas.
3. Type-III kerogen (gas-prone material) consists of humic, coaly material generated from terrestrial higher plants. Orange or brown, translucent, phytoclasts and structureless materials, woody fragments are typical. This kind of kerogen produces only gas.

4. Type IV kerogen is a secondary type of kerogen; practically it contains only aromatic compounds; the carbonization of organic matter was carried out through the combustion/natural pyrolysis and /or oxidation (pre-depositional) processes; it presents non-potential to hydrocarbon production.

Samples Nos. 1, 2, 4 and 7 are characterized by the presence of opaque and non-opaque phytoclasts and sporomorphs (Fig. 11). On the other hand, sample No. 5 consists predominantly amorphous organic matter in addition to a few amounts of non-opaque phytoclasts and a rare amount of sporomorphs (Fig. 11). Vitrinite particles large enough to measure are common (except sample No. 5 is moderate) and exhibit range of reflectance values (Table 5). Plant spores are present as a good indicator of thermal maturity throughout the oil window. The dark brown color of the palynomorphs in the microphotographs (Fig. 11) suggests TAI value of about 3.1-3.3 on the Chevron Scale (Table 9) and it can be correlated to many other maturity scales as Spore Coloration Index (SCI), as seen in the same table. These data suggest the OM in these samples has reached the peak generation stage of thermal maturity for oil prone OM, and pass to the post generation stage of thermal maturity for oil prone as in (Sample No. 7). From the previous data the kerogen type is mainly type III (gas-prone) and/or IV which is characterized by major terrestrial input of organic material.

4. Conclusions

The shale of Magharet El Maiah Formation, southwestern Sinai, is enriched with kaolinite with respect to montmorillonite and illite with some inclusion of quartz and pyrite indicating oxic terrestrial depositional condition. The chemical composition show the prevailing of SiO_2 and Al_2O_3 supporting the clay mineralogy of samples. The elevated LOI is indicating the relatively elevated organic matter and clay minerals within the samples. The content of heavy metals within the samples was of moderatelyenriched as indicated from the pollution indices. However the appearance good hydrocarbon source as indicated by the high TOC, the generative potentiality of these sediments was of poor hydrocarbon potentiality with IV kerogen type (gas prone).

Sample No.	Major Visual Kerogen analysis
1	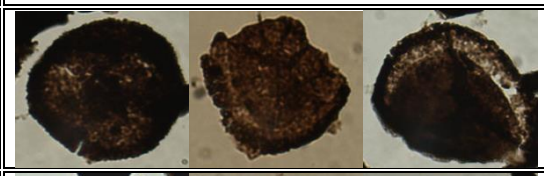
2	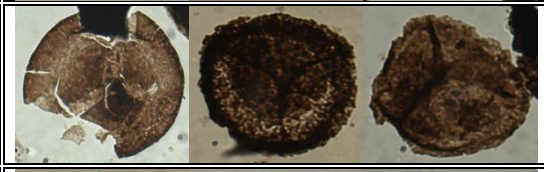
4	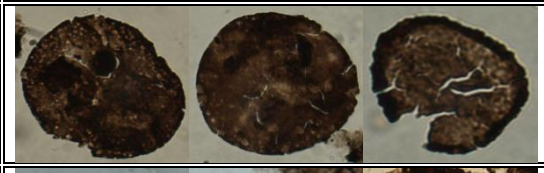
5	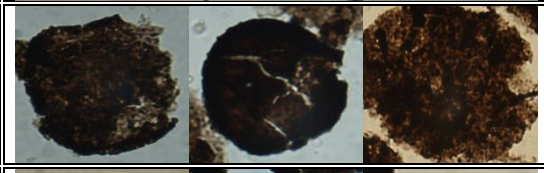
7	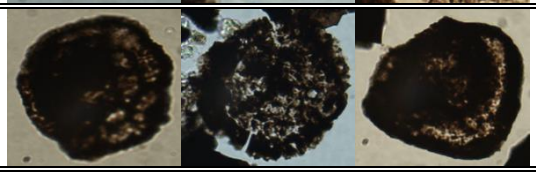

Fig. 11:Microscopic Plates showing Visual kerogen types.

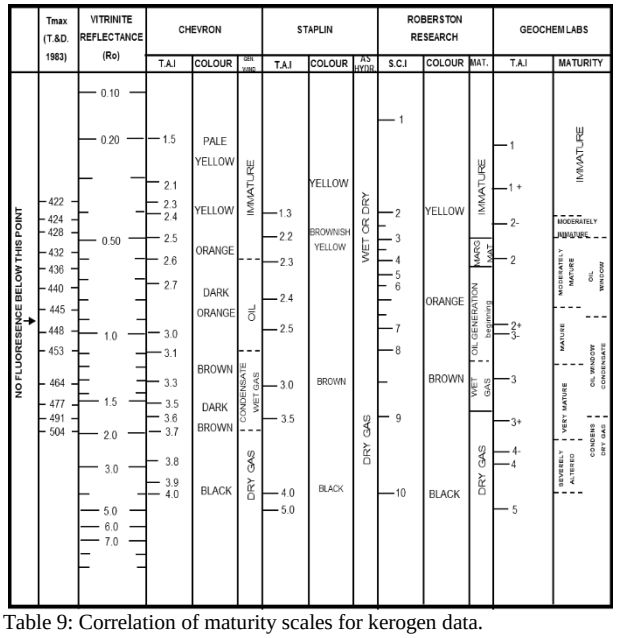

Table 9: Correlation of maturity scales for kerogen data.

Conflicts of interest

There are no conflicts to declare

Formatting of funding sources

This paper is based upon work supported by Science, Technology & Innovation Funding Authority (STDF) under grant (26190), and so many thanks for STDF for their support.

Acknowledgment

The authors would like to thank The Geological Sciences Dept., National Research Centre and Stratochem services, Egypt for facilitates during this work.

References

[1] AAPG (American Association of Petroleum Geologists, Energy Minerals Division), Unconventional Energy Resources: 2017 Review. Nat Resour Res 28: 1661–1751 (2019). https://doi.org/10.1007/s11053-018-9432-1

[2] Xie X, Li M, Xu J, Snowdon LR, Volkman JK., Geochemical characterization and artificial thermal maturation of kerogen density fractions from the Eocene Huadian oil shale, NE China. Organic Geochemistry 144, 103947 (2020).

[3] Zhang T, Wang X, Zhang J, Sun X, Milliken KL, Ruppel SC, Enriquez D., Geochemical evidence for oil and gas expulsion in Triassic lacustrine organic-rich mudstone, Ordos Basin, China. Interp. 5, SF41–SF61 (2017).

[4] Shao D, Zhang T, Ko LT, Li Y, Yan J, Zhang L, Luo H, Qiao B., Experimental investigation of oil generation, retention, and expulsion within Type II kerogen-dominated marine shales: Insights from gold-tube nonhydrous pyrolysis of Barnett and Woodford Shales using miniature core plugs. International Journal of Coal Geology 217: 103337 (2020).

[5] Berlendis S, Beyssac O, Derenne S, Benzerara K, Anquetil C, Guillaumet M, Estève I, Capelle B, Comparative mineralogy, organic geochemistry and microbial diversity of the Autun black shale and Graissessac coal (France). International Journal of Coal Geology 132: 147–157 (2014)

[6] Peters, K.E., Guidelines for evaluating petroleum source rock using programmed pyrolysis. Am. Assoc. Petrol. Geol. Bull. 70, 318–329 (1986), https://doi.org/10.1306/ 94885688-1704-11D7-8645000102C1865D.

[7] Tissot BP, WelteDH., Petroleum Formation and Occurrence 2nd (Ed.) Springer-Verlag, New York, 699p (1984).

[8] Liu B, Teng J, Mastalerz M, Schieber J, Assessing the thermal maturity of black shales using vitrinite reflectance: Insights from Devonian black shales in the eastern United States. Intern. J. Coal Geol. 220: 103426 (2020), https://doi.org/10.1016/j.coal.2020.103426

[9] Temraz MG, Mineralogical and Geochemical Studies of Carbonaceous Shale Deposits from Egypt. M.Sc. Thesis, Department of Civil Engineering and Applied Geoscience, Technical University of Berlin, Berlin, Germany (2005).

[10] Mostafa AR, Younes MA., Significance of organic matter in recording paleoenvironmental conditions of the Safa Formation coal sequence, Maghara area, North Sinai, Egypt. Intern. J. Coal Geol. 47: 9-21 (2001).

[11] Ghandour IM, Harue M, Wataru M., Mineralogical and chemical characteristics of Bajocian-Bathonian shales, G. Al-Maghara, North Sinai, Egypt: Climatic and environmental significance. Geochemical J 37: 87-108 (2003).

[12] El-Kelani A, Contribution to the geology of the Paleozoic in Sinai. Ann. the Geol. Surv.Egy. XXIV: 233-255 (2001).

[13] Soliman SM, EI-Fetouh M., Lithostratigraphy of the Carboniferous Nubian type sandstones in westcentral Sinai. Egyptian J. Geology, 13: 61-143(1969).

[14] El Aassy IE, Ahmed FY, Mohammed GA, Al Shami AS, Gabr MM, Rabboh AA, New resource of rare earth elements in Sinai, Egypt. 7th Intern. Conf. on Geochemistry, Fac. Sci, Alex, Egypt,. V. III: 177-184 (2006).

[15] El Aassy I.E, Botros NH, Abdel Razik A, Sherif H, Al Moafy A, Aita S, El Terb R, Al Shami AS, Report on the Prospection and Proving of Some Radioactive Occurrences in West Central Sinai, Egypt", Internal Report, Nuclear Materials Authority, Cairo (1986).

[16] Muller G., Schwermetalle in den Sedimenten des Rheins, VeranderungemSeit 1971.Umschau 79:778-783 (1979).

[17] Sutherland RA., Bed sediment-associated trace metals in an urban stream, Oahu, Hawaii. Environmental Geology, 39(6): 611–627 (2000).

[18] Hakanson L., An Ecological Risk Index for Aquatic Pollution Control: A Sedimentological Approach. Water Res. 14: 975-1001 (1980).

[19] Tomlinson DL, Wilson JG, Harris CR, Jeffney DW., Problems in the assessment of heavy metal levels in estuaries and the formation of a pollution index. Helgol.Meeresunters, 33: 566-572 (1980).

[20] Taylor SR, McLennan SM, The Continental Crust: Its Composition and Evolution. Blackwell, Oxford (1985).

[21] Bam EKP, Akiti TT, Osea SD, Ganyaglo SY, Gibrilla A., Multivariate cluster analysis of some major andtrace elements distribution in an un-saturated zone profile, Densu river Basin, Ghana. Afr. J. Environ. Sci. Technol. 5: 155-167 (2011).

[22] Yahya MMA, Hakimi MH, Galmed MA, El-Sabrouty MN, Ibrahim YKH, Paleoenvironmental and paleoclimatic conditions during the deposition of the bauxite layer (Upper Cretaceous) using multi-proxy geochemical and palynological analyses, in the Zabirah Area, Northern Saudi. Arab. J Geosci 11: 15 (2018), https://doi.org/10.1007/s12517-017-3379-0

[23] Abou El-Anwar EA, El-Sayed MS., Composition of black shale from Quseir, Red Sea, Egypt with emphasis on the sequential extraction of some metals. Bulletin of the National Research Centre 32(109):131 (2008).

[24] Abou El-Anwar EA Mineralogical, petrographical, geochemical, diageneses and provenance of the Cretaceous Black Shales, Duwi Formation at Quseir-Safaga, Red Sea, Egypt. Egypt. J. Petrol. 26: 915-926 (2017).

[25] Abou El-Anwar EA, Mekky HS, Abdel Wahab W., P2O5- F- U Characterization and Depositional Environment of Phosphatic Rocks for the Duwi Formation, Qussier- Safaga Region, Red Sea Coast, Egypt, Egypt.J.Chem. 62(12): 1-12 (2019a).

[26] Abou El-Anwar EA, Mekky HS, Abdel Wahab W., Geochemistry, mineralogy and depositional environment of black shales of the Duwi Formation, Qusseir area, Red Sea coast, Egypt. Carbonates and Evaporites 34: 883-892 (2019b).

[27] Ross DJK, Bustin RM Investigating the use of sedimentary geochemical proxies for palaeoenvironment interpretation of thermally mature organic-rich strata: examples from the Devonian– Mississippian shales, Western Canadian Sedimentary Basin. ChemGeol 260(1-2):1–19 (2009).

[28] Rudnick RL, Gao S., Composition of the Continental Crust. Treatise on Geochemistry 4: 1-51(2014). https://doi.org/10.1016/B978-0-08-095975-7.00301-6.

[29] Wenger LM, Isaksen GH, Controls of hydrocarbon seepage intensity on level of biodegradation in sea bottom sediments. Org Geochem 12:1277–1292 (2002).

[30] Ratcliffe KT, Wright AM, Montgomery P, Palfrey A, Vonk A, Vermeulen J, Barrett M, Application of chemostratigraphy to the Mungaroo Formation, the orgoneld, offshore Northwest Australia. Australian Petroleum Production and Exploration Association Journal (50th Anniversary Issue), 371–388 (2010).

[31] Pi DH, Jiang SY, Luo L, Yang JH, Hong-Fei Ling HF., Depositional environments for stratiform witherite deposits in the Lower Cambrian black shale sequence of the Yangtze platform, southern Qinling region, SW China: evidence from redox-sensitive trace element geochemistry. Palaeogeogr Palaeoclimatol Palaeoecol, 398: 125-131 (2014).

[32] Adegoke AK, Abdullah WH, Hakimi MH, Yandoka BM, Mustapha KA, Aturamu AO., Trace elements geochemistry of kerogen in Upper Cretaceous sediments, Chad (Bornu) Basin, northeastern Nigeria: origin and paleo-redox conditions. J Afr. Earth Sci 100: 675-683 (2014).

[33] Pattan JN, Pearce NJG, Bottom water oxygenation history in southeasternArabian Sea during the past 140 ka: results from redox-sensitive elements.Palaeogeogr. Palaeoclimatol.Palaeoecol.280, 396–405 (2009).

[34] Lewan MD, Factors controlling the proportionality of vanadium to nickel incrude oils. Geochim.Cosmochim.Acta 48, 2231–2238 (1984).

[35] Singh M, Sharma M, Tobschall HL., Weathering of the Ganga alluvial plain, northern India: implications from fuvial geochemistry of the Gomati River. Appl Geochem 20: 1–21 (2005).

[36] Nesbitt HW, Young GM., Early Proterozoic climates and plate motion inferred from major element chemistry of lutites. Nature 299 :715-717 (1982).

[37] Kuşcu M, Özsoy R, Özçelik O, Altunsoy M., Trace and rare earth element geochemistry of black shales in Triassic Kasımlar Formation, Anamas-Akseki Platform, Western Taurids, Turkey. IOP Conf. Series: Earth and Environmental Science 44: 042012 (2016).

[38] Hu F, Liu Z, Meng Q, Song Q, Xie W., Characteristics and comprehensive utilization of oil shale of the Upper Cretaceous Qingshankou Formation in the southern songliao basin, NE China. Oil Shale, 34(4): 312-335 (2017).

[39] Armands G., Geochemical studies of uranium, molybdenum and vanadium in a Swedish alum Shale. Stockholm Contrib.Geol.27, 148 p (1972).

[40] Tourtelot HA., Black shale-its deposition and diagenesis. Clays and Clay Minerals, 27, 313-321 (1979).

[41] Holland HD., Metals in black shales-a reassessment. Econ Geol. 74: 295-314 (1979).

[42] Jr Coveney RM, Murowchick JB, Grauch RI, Michael D, Glascock D, Denison JD., Gold and platinum in shales with evidence against extraterrestrial sources of metals. Chem Geol. 99: 101-114 (1992).

[43] Jiang SY, Yang JH, Ling HF, Feng HZ, Chen YQ, Chen JH., Re–Os isotopes and PGE geochemistry of black shales and intercalated Ni–Mo polymetallic sulfide bed from the Lower Cambrian Niutitang Formation, South China,"Progress in Natural Sciences 13: 788-794 (2003).

[44] Abou El-Anwar EA, Samy YM., Salman SA., Heavy metals hazard in Rosetta Branch sediments, Egypt. J. Mater. Environ. Sci. 9(7): 2142-2152 (2018).

[45] Abou El-Anwar EA., Assessment of heavy metal pollution in soil and bottom sediment of Upper Egypt: comparison study. Bulletin of the National Research Centre, 43:180 (2019c), https://doi.org/10.1186/s42269-019-0233-4

[46] Elnazer AA, Salman SA, Seleem EM, Abu El Ella EM., Assessment of some heavy metals pollution and bioavailability in roadside soil of Alexandria-MarsaMatruh Highway, Egypt. International Journal of Ecology 2015, Article ID 689420, 7 pages, (2015) doi:10.1155/2015/689420

[47] Mekky HS, Abou El-Anwar EA, Salman SA, Elnazer AA, Abdel Wahab W, Asmoay AS., evaluation of heavy metals pollution by using pollution indices in the Soil of Assiut District, Egypt. Egyptian Journal of Chemistry 62(9): 1673-1683 (2019).

[48] Alexander, T., Baihly, J., Boyer, C., Clark, B., Waters, G., Jochen, V., Calvez, J.L., Lewis, R., Miller, C.K., Thaeler, J., Gas shale revolution. Oilfield Rev. 23, 40–55 (2011).

[49] Gromet LP, Haskin LA, Korotev RL, Dymek RF., The North American shale composite: its compilation, major and trace element characteristics. Geochim.Cosmochim.Acta 48: 2469–2482 (1984).

[50] Turekian KK, Wedepohl KH., Distribution of the elements in some major units of the earth's crust. Geol. Soc. Am. Bull. 72, 175–192 (1961).

[51] Vine JD, Tourtelot EB., Geochemistry of black shale deposits; a summary report. Econ.Geol. 65, 253–272 (1970).

[52] Ketris M, Yudovich YE., Estimations of Clarkes for carbonaceous biolithes: world averages for trace element contents in black shales and coals. Int. J. Coal Geol. 78: 135–148 (2009).

[53] Peters KE, Cassa MR., Applied source rock geochemistry, The Petroleum System-From Source to Trap. AAPG Memoir 60: 93-120 (1994).

[54] Hunt JM., Petroleum Geochemistry and Geology, 2nd edition Freeman and company, New York, 743 p (1996).

[55] Berner RA, Raiswell R., Burial of organic carbon and pyrite sulfur in sediments over Phanerozoic time: a new theory: Geochimica et Cosmochimica Acta, 47: 855- 862 (1983).

[56] Owusu EB, Tsegab H, Sum CS, Padmanabhan E, Organic geochemical analyses of the Belata black shale, Peninsular Malaysia; implications on their shale gas potential. Journal of Natural Gas Science and Engineering 69: 102945 (2019), https://doi.org/10.1016/j.jngse.2019.102945

[57] Hunt J M., Petroleum geochemistry and geology. New York, W. H. Freeman, 743p (1995).

[58] Dahl B, Bojesen-Koefoed J, Holm A, Justwan H, Rasmussen E, Thomsen E., A new approach to interpreting Rock-Eval S2 and TOC data for kerogen quality assessment, Organic Geochemistry 35: 1461-1477 (2004).

[59] Tissot B, Durand B, Espitalie J, Compaz A., Influence of nature and diagenesis of organic matter in formation of petroleum. AAPG Bull. 58(3): 499-506 (1974).

[60] Ghori KAR., Petroleum source-rock potential and thermal history of the officer Basin, Western Australia, West AustGeolSurv, p 52 (1998).

[61] Tissot BP, Welte DH., Petroleum formation and occurrence. Springer, Verlag, Berlin, Heidelberg. New York,pp. 538 (1978).

[62] Pitman JK, Franczyk KJ, Anders DE., Marine and NonmarineGas-Bearing Rocks in Upper Cretaceous Blackhawk and Neslen Formations, Eastern Uinta Basin, Utah - Sedimentology, Diagenesis, and Source Rock Potential. AAPG Bulletin, 71: 76-94 (1987).

[63] Espitalie J, Laporte L, Madec M, Marquis F, Leplat P, Paulet J, Boutefeu A., Methode rapid de caracterisation des rocks meres, de leur potential petrolier et leur degree devolution. Rev. Inst. Fr. Petrol. 32: 23-42 (1977).

[64] Espitalie J, Deroo G, Marquis F., Rock-Eval pyrolysis and its application. Inst. Fr.Preprint, 33578, 72p (1985).

[65] Peters KE, Moldowan JM, Schoell M, Hempkins WB., Petroleum isotopicand biomarker composition related to source rock organic matter and depositional Environment. Organic Geochemistry 10: 17-27 (1986).

[66] Tissot BP, Pelet R, Ungerer P., Thermal history of sedimentary basins, maturation indexes, and kinetics of oil and gas generation, AAPG Bulletin 71: 1445-1466 (1987).

[67] Waples DW., Geochemistry in Petroleum Exploration. International Human Resources Development Corporation, Boston, 232 p (1985).

[68] Manning DAC., Organic Geochemistry: Advances and Applications in the Natural Environment: Advances and Applications in Energy and the Natural Environment Manchester University Press, Manchester, UK, 480 p, Netherlands, 153-191 (1991).

[69] McCartney JT, Teichmüller M, Classification of coals according to degree of coalification by reflectance of the vitrinite component. Fuel 51, 64–68 (1972).

[70] Espitalié J, Bordenave ML., Source rock parameters. In: Bordenave, M.L. (Ed.), Applied Petroleum Geochemistry, Technip, Paris, pp. 219-225 (1993).

[71] Langford FF, Blank-Valleron MM., Interpretation of Rock-Eval pyrolysis data using pyrolyzable hydrocarbons vs. total organic carbon AAPG Bulletin, 76: 799-804 (1990).

[72] Tyson RV., Sedimentary OrganicMatter-Organic Facies and Palynofacies. Chapman & Hall, London, 615p (1995).

[73] Tyson RV., Palynofacies analysis. In: Applied Micropaleontology, Jenkins, D.G. (Ed.), Kluwer Academic Publishers. The Netherlands, Amsterdam, pp. 153-191 (1993).